

Figure 3. Molar proton liberation, $\delta(H^+)/\delta C_M$, and its relationship to \bar{n} and \bar{n}_H for the Ni(II)/GHA system.

Consequently, some protons will already have dissociated from the ligand before complexation. The above data show that coordination of Ni(II) by these amino hydroxamic acids involves coordination from the amino and NHO^- groups and does not involve the carbonyl in agreement with our previous conclusions on the Fe(III)/GHA system in solution.¹⁵ Aqueous solutions of both the Ni(II)/GHA and Ni(II)/SHA systems are diamagnetic over a wide pH range, suggesting a square-planar configuration for the NiA_2 species in solution as well as in the solid state. The solution electronic spectra

provide further confirmation of this configuration since both systems show two bands, one in the 370–430-nm region and one in the 490–510-nm region assigned respectively as $^1A_{1g} \rightarrow ^1A_{2g}$ and $^1A_{1g} \rightarrow ^1B_{1g}$ transitions in square-planar symmetry by comparison with observed spectra of Ni(II) complexes of confirmed square-planar configuration.¹⁸ Infrared spectra were measured in D_2O in order to investigate further the role of the ketonic oxygen in coordination to nickel in solution. Shifts of about 30 cm^{-1} occur, comparing nickel solutions of pD values corresponding to a predominance of the MA_2 species and the free ligand, respectively; however, these shifts are concentration dependent and so most probably arise from intermolecular H bonding between the carbonyl group of one complex and the hydrogen of an adjacent NHO^- group, similar to that observed in the solid-state structure of $Ni(GHA)_2$,¹⁷ rather than from coordination to the metal. It thus appears from both the species distribution and the solution structural studies that, at least for $Ni(GHA)_2$, the solid-state structure persists in solution.

Registry No. $Ni(AHA)_2 \cdot 2H_2O$, 85749-06-0; $Ni(PHA)_2 \cdot 2H_2O$, 85749-07-1; $Ni(GHA)_2$, 83267-42-9; $Ni(SHA)_2$, 85749-08-2; AHA, 546-88-3; PHA, 2580-63-4; GHA, 5349-80-4; SHA, 31697-35-5.

Supplementary Material Available: Tables of sample compositions and figures showing proton displacement and species distribution (11 pages). Ordering information is given on any current masthead page.

(18) Lever, A. B. P. "Inorganic Electronic Spectroscopy"; Elsevier: New York, 1968.

Contribution No. 795 from the Charles F. Kettering Research Laboratory, Yellow Springs, Ohio 45387, and Department of Chemistry, Northwestern University, Evanston, Illinois 60201

Synthesis, Characterization, and EPR Spectral Studies of the Multimetal Species $[Fe(MS_4)_2]^{3-}$ (M = Mo, W)

G. DELBERT FRIESEN,[†] JOHN W. McDONALD,^{*†} WILLIAM E. NEWTON,[†] WILLIAM B. EULER,[‡] and BRIAN M. HOFFMAN^{*‡}

Received November 19, 1982

The complexes $[Et_4N]_3[Fe(MS_4)_2]$ (M = Mo, W) have been prepared by reaction of $[Et_4N]_2MS_4$ with $Fe(S_2CNC_5H_5)_2$ in CH_2Cl_2 and routinely characterized by infrared and visible spectroscopy. Cyclic voltammetry studies show that, for M = Mo, only the 3-/4- couple is reversible but that, for M = W, reversible 1-/2-, 2-/3-, and 3-/4- couples are observed. The complexes exhibit magnetic moments consistent with the presence of three unpaired electrons, prompting low-temperature electron paramagnetic resonance studies. Signals that are consistent with an $S = 3/2$ spin state are observed in a variety of solvents for both M = Mo and M = W, and the absence of high-field resonances is indicative of a relatively high value for the zero-field splitting parameter. Values of $\lambda = E/D$ are estimated for all systems. The potential significance of the similarity of the EPR spectra of these complexes to those of the molybdenum-iron protein of nitrogenase and its cofactor is discussed.

Introduction

The presence of a unique iron-molybdenum-sulfur moiety in the iron-molybdenum protein ($[Mo-Fe]$) of the enzyme nitrogenase has been implicated by X-ray absorption,¹ EPR,² and Mössbauer,^{2b,c} spectroscopic studies. Additional studies⁴ have now shown that this Fe-Mo-S entity can apparently be extracted intact into *N*-methylformamide after denaturation of the protein. The extracted unit is called the iron-molybdenum cofactor (FeMo-co), and its stability in this organic medium bodes well for attempts to prepare a synthetic analogue for the molybdenum site of nitrogenase. These findings have prompted the recent syntheses of complexes containing

these three elements as well as others where tungsten has been substituted for molybdenum. These species are all derived

- (1) (a) Cramer, S. P.; Hodgson, K. O.; Gillum, W. O.; Mortenson, L. E. *J. Am. Chem. Soc.* **1978**, *100*, 339. (b) Cramer, S. P.; Gillum, W. O.; Hodgson, K. O.; Mortenson, L. E.; Stiefel, E. I.; Chisnel, J. R.; Brill, W. J.; Shah, V. K. *Ibid.* **1978**, *100*, 3814. (c) Burgess, B. K.; Yang, S.-S.; You, C. B.; Li, J.-G.; Friesen, G. D.; Pan, W.-H.; Stiefel, E. I.; Newton, W. E.; Conradson, S. D.; Hodgson, K. O. "Current Perspectives in Nitrogen Fixation"; Gibson, A. H.; Newton, W. E., Eds.; Elsevier/North Holland: New York, 1981; p 71.
- (2) (a) Palmer, G.; Multani, J. S.; Cretney, W. D.; Zumft, W. G.; Mortenson, L. E. *Arch. Biochem. Biophys.* **1972**, *153*, 325. (b) Münck, E.; Rhodes, H.; Orme-Johnson, W. H.; Davis, L. C.; Brill, W. J.; Shah, V. K. *Biochim. Biophys. Acta* **1975**, *400*, 32. (c) Zimmerman, R.; Münck, E.; Brill, W. J.; Shah, V. K.; Henzl, M. T.; Rawlings, J.; Orme-Johnson, W. H. *Ibid.* **1978**, *537*, 185. (d) Huynh, B. H.; Henzl, M. T.; Christner, J. A.; Zimmerman, R.; Orme-Johnson, W. H.; Münck, E. *Ibid.* **1980**, *623*, 124.

[†] Charles F. Kettering Research Laboratory.

[‡] Northwestern University.

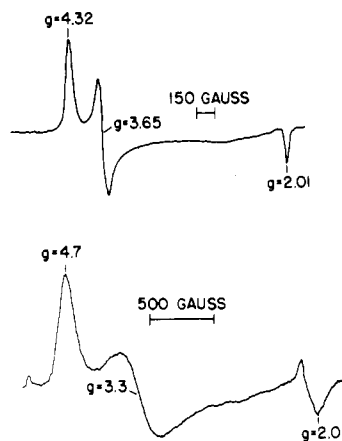


Figure 1. EPR spectra of the iron-molybdenum protein of nitrogenase (top) in aqueous media and the iron-molybdenum cofactor (bottom) in *N*-methylformamide.

from reactions involving the tetrathiometalates (MS_4^{2-} ; M = Mo, W) and can be roughly divided into two groups: (A) those containing an FeS_2M linkage(s), i.e., MS_4^{2-} behaving as a bidentate ligand to iron; and (B) those containing Fe_3MoS_4 cubane-type units. Some examples^{3,5-7} of type A species are $[Cl_2FeS_2MS_2]^{2-}$, $[Cl_2FeS_2MS_2FeCl_2]^{2-}$, $[(PhS)_2FeS_2MS_2]^{2-}$, and $[(PhS)_2FeS_2FeS_2MoS_2]^{3-}$ while type B complexes include $[Fe_6Mo_2S_9(SR)_8]^{3-}$, $[Fe_6Mo_2S_8(SR)_9]^{3-}$, and $[Fe_7Mo_2S_8(SR)_{12}]^{3-}$. In recent reviews,⁸ the spectral and structural properties of some of these compounds are summarized and the species evaluated as potential synthetic analogues for the molybdenum site of nitrogenase.

As part of our program in this area, we recently reported⁹ briefly on the synthesis and characterization of the new Fe-Mo-S species $[Fe(MoS_4)_2]^{3-}$ (**1**) and described a few of its spectral and electrochemical properties. Almost simultaneously, Coucouvanis and co-workers¹⁰ published an X-ray structural determination of this compound, which had been prepared independently by a method similar to ours, and they later presented Mössbauer studies of the compound.^{10b} Their study confirmed our postulated stoichiometry for **1** and provided bond length data around molybdenum which could be compared with that determined by X-ray absorption spectroscopic studies¹ on the iron-molybdenum protein of nitrogenase. In general, the Mo-S and Mo-Fe distances of the

cubane-type complexes are more similar to those of $[Mo-Fe]$ (but not an exact fit) than these distances in the linear species, **1** included.

The magnetic properties of **1** were particularly intriguing because of their similarity to $[Mo-Fe]$. Susceptibility measurements indicated that the complex contained three unpaired electrons, and the EPR spectrum of **1** in frozen MeCN solution at low temperature was characteristic of an $S = 3/2$ spin state exhibiting apparent *g* values at 5.2, 2.7, and 1.8. In fact, the dithionite-reduced forms of $[Mo-Fe]$ and its cofactor ($FeMo-co$) both have EPR spectra (Figure 1) which are similar in form to that of **1** (see below) and are generally thought to be due to an $S = 3/2$ spin state.² These data suggested the need for a more detailed EPR spectral study of **1** in order to more carefully assess the significance of this similarity.

Herein we fully describe the synthetic procedure for the preparation of **1** and for its tungsten analogue $[Fe(WS_4)_2]^{3-}$ (**2**), and the physicochemical properties of these complexes are detailed with particular emphasis on EPR spectral studies in a number of solvents. Finally, the potential worth of these complexes as synthetic analogues for the molybdenum site of nitrogenase is discussed.

Experimental Section

Materials and Methods. All reactions were carried out under an inert atmosphere of argon by using standard techniques. Solvents were treated as follows prior to use and then degassed: CH_2Cl_2 , dried over molecular sieves; NMF, stirred over $NaHCO_3$ and distilled under reduced pressure; MeCN, distilled from CaH_2 ; DMF, Burdick and Jackson, used as received; diethyl ether, Mallinckrodt, used as received. $(NH_4)_2MoS_4$, $(NH_4)_2WS_4$, and $Fe(S_2CNC_5H_{10})_2$ were prepared as previously described.¹¹⁻¹³

Infrared spectra were recorded on a Beckman IR-20A spectrophotometer and UV-vis spectra on a Cary 118C instrument. At CFKRL, EPR spectra were obtained with a Varian Associates 4502 spectrometer equipped with a Model V4560 100-kHz modulation control unit, an X-band microwave bridge, and a Hewlett-Packard X532 G frequency meter. Cooling was via liquid-He boil-off using an Air Products transfer line and associated equipment. At Northwestern University, EPR spectra were obtained at 4.2 K on a modified Varian E-4 X-band spectrometer. Frequencies were measured by a transfer oscillator, and the field was calibrated with DPPH ($g = 2.0036$). EPR spectra studied here could be analyzed in terms of the spin Hamiltonian for an $S = 3/2$ system (eq 1), where $\lambda = E/D$, E

$$\hat{H} = [g_x H_x \hat{S}_x + g_y H_y \hat{S}_y + g_z H_z \hat{S}_z] + D[(\hat{S}_z^2 - 5/4) + \lambda(\hat{S}_x^2 - \hat{S}_y^2)] \quad (1)$$

and *D* are respectively the rhombic and tetragonal zero-field-splitting components, and the g_i are the principal components of the *g* tensor. The parameter λ has as its physically meaningful range $0 < \lambda < 1/3$, with $\lambda = 0$ corresponding to a tetragonal system and $\lambda = 1/3$ to the maximum rhombic distortion.¹⁴ Where appropriate, spectral analyses were corroborated by computer simulations using program SIM 14.¹⁵

Cyclic voltammetric experiments were carried out with a setup composed of a PAR Model 73 potentiostat, a Hewlett-Packard 3310B function generator, an Explorer digital oscilloscope from the Nicolet Instrument Corp., and an MFE 815 X-Y recorder. The platinum-button working electrode was separated from the reference electrode (SCE) by fine-porosity frits and a bridge containing solvent and supporting electrolyte (0.1 M $[Bu_4N]BF_4$). The auxiliary electrode of platinum mesh was immersed in electrolyte solution and isolated from the bulk solution by a frit. $[Bu_4N]BF_4$ was purchased from Eastman and used as received. Typically, the scan rate was 0.5 V/s.

Magnetic susceptibility measurements were made by the Evans method using a Varian A-60 NMR spectrometer. Elemental analyses

- (3) (a) Coucouvanis, D.; Baenziger, N. D.; Simhon, E. D.; Stremple, P.; Swenson, D.; Simpopoulos, A.; Kostikas, A.; Petrouleas, V.; Papaefthymiou, V. *J. Am. Chem. Soc.* **1980**, *102*, 1732. (b) Tieckelmann, R. H.; Silvis, H. C.; Kenut, T. A.; Huynk, B. H.; Waszczak, J. V.; Teo, B.-K.; Averill, B. A. *Ibid.* **1980**, *102*, 5550. (c) Müller, A.; Jostes, R.; Tölle, H. G.; Trautwein, A.; Bill, E.; *Inorg. Chim. Acta* **1980**, *46*, L121.
- (4) (a) Shah, V. K.; Brill, W. J. *Proc. Natl. Acad. Sci. U.S.A.* **1977**, *74*, 3249. (b) Rawlings, J.; Shah, V. K.; Chisnell, J. R.; Brill, W. J.; Zimmerman, R.; Münck, E.; Orme-Johnson, W. H. *J. Biol. Chem.* **1978**, *253*, 1001. (c) Burgess, B. K.; Stiefel, E. I.; Newton, W. E. *Ibid.* **1980**, *255*, 1001.
- (5) Coucouvanis, D.; Simhon, E. D.; Swenson, D.; Baenziger, N. C. *J. Chem. Soc., Chem. Commun.* **1979**, 361.
- (6) Tieckelmann, R. H.; Averill, B. A. *Inorg. Chim. Acta* **1980**, *46*, L35.
- (7) (a) Wolff, T. E.; Power, P. P.; Frankel, R. B.; Holm, R. H. *J. Am. Chem. Soc.* **1980**, *102*, 4694. (b) Christou, G.; Garner, C. D.; Mabbs, F. E.; Kings, T. J. *J. Chem. Soc., Chem. Commun.* **1978**, 740.
- (8) (a) Stiefel, E. I. "Molybdenum and Molybdenum-Containing Enzymes"; Pergamon Press: New York and Oxford, 1980; p 41. (b) Newton, W. E.; McDonald, J. W.; Friesen, G. D.; Burgess, B. K.; Conradson, S. D.; Hodgson, K. O. "Current Perspectives in Nitrogen Fixation"; Gibson, A. H., Newton, W. E., Eds.; Elsevier/North Holland Press: New York, 1981; p 30.
- (9) McDonald, J. W.; Friesen, G. D.; Newton, W. E. *Inorg. Chim. Acta* **1980**, *46*, L79.
- (10) (a) Coucouvanis, D., private communication. Coucouvanis, D.; Simhon, E. E.; Baenziger, N. C. *J. Am. Chem. Soc.* **1980**, *102*, 6644. (b) Simpopoulos, A.; Papaefthymiou, V.; Kostikas, A.; Petrouleas, V.; Coucouvanis, D.; Simhon, E. D.; Stremple, P. *Chem. Phys. Lett.* **1981**, *81*, 261.

- (11) Krüss, G. *Justus Liebigs Ann. Chem.* **1884**, *225*, 6.
- (12) Corleis, E. *Justus Liebigs Ann. Chem.* **1886**, *232*, 264.
- (13) de Vries, J. L. K. F.; Trooster, J. M.; de Boer, E. *Inorg. Chem.* **1973**, *12*, 2730.
- (14) Abragam, A.; Bleaney, B. "EPR of Transition Ions"; Oxford University Press: London, 1970.
- (15) Lozos, G. P.; Hoffman, B. M.; Franz, C. Quantum Chemistry Program Exchange, Program 256, Indiana University, Bloomington, IN, 1972; SIM 14.

for CHN were performed at CFKRL with a Perkin-Elmer 240 instrument equipped with a Microjector from Control Equipment Corp. Iron, molybdenum, and tungsten analyses were carried out at CFKRL by standard techniques and sulfur analyses by Galbraith Laboratories, Knoxville, TN.

Preparation of Complexes. $[\text{Et}_4\text{N}]_2\text{MoS}_4$. $(\text{NH}_4)_2\text{MoS}_4$ (20 g) was dissolved in 230 mL of a 10% solution of $[\text{Et}_4\text{N}]\text{OH}$ in H_2O . The solution was pumped on for 2 h to remove NH_3 ; then the reaction mixture was filtered. Addition of isopropyl alcohol (400 mL) to the filtrate caused the separation of the product, which was isolated by filtration, washed with isopropyl alcohol and diethyl ether, and dried in vacuo. The yield was 25 g, 68%. The purity of the powdery compound was shown to be high by both infrared and electronic spectral analysis. If desired, the product can be recrystallized from hot MeCN but this is normally not necessary.

$[\text{Et}_4\text{N}]_2\text{WS}_4$. This compound was prepared by the same method as its molybdenum analogue using 11 g of $(\text{NH}_4)_2\text{WS}_4$ and 94 mL of 10% $[\text{Et}_4\text{N}]\text{OH}$ in H_2O . The yield was 12.5 g, 60%. Purity was determined by spectral (IR, UV-vis) analysis.

$[\text{Et}_4\text{N}]_3[\text{Fe}(\text{MoS}_4)_2]$. The solid compounds $\text{Fe}(\text{S}_2\text{CNC}_5\text{H}_{10})_2$ (1.50 g; 3.99 mmol) and $[\text{Et}_4\text{N}]_2\text{MoS}_4$ (4.50 g; 9.30 mmol) were slurried in CH_2Cl_2 (80 mL). After being stirred at ambient temperature for 1.5 h, the reaction mixture was filtered and the solid product washed with CH_2Cl_2 , acetone, H_2O , and acetone and then dried in vacuo. The yield was 1.33 g, 37%. The solid was recrystallized from MeCN/ Et_2O to yield analytically pure product. Anal. Calcd for $\text{C}_{24}\text{H}_{60}\text{N}_3\text{FeMo}_2\text{S}_8$: C, 32.2; H, 6.71; N, 4.70; Fe, 6.26; Mo, 21.5; S, 28.6. Found: C, 32.0; H, 6.78; N, 4.59; Fe, 6.22; Mo, 20.8; S, 29.0.

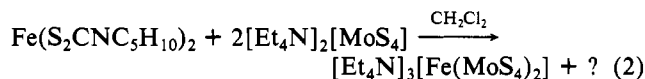
$[\text{Et}_4\text{N}]_3[\text{Fe}(\text{WS}_4)_2]$. The solid compounds $\text{Fe}(\text{S}_2\text{CNC}_5\text{H}_{10})_2$ (0.40 g; 1.06 mmol) and $[\text{Et}_4\text{N}]_2\text{WS}_4$ (1.05 g; 1.83 mmol) were slurried in a biphasic mixture of CH_2Cl_2 (35 mL) and H_2O (5 mL). After being stirred at ambient temperature for 1.5 h, the reaction mixture was filtered and the product sucked as dry as possible and then washed with acetone. After drying in vacuo, the yield was 0.54 g, 48%. The solid was recrystallized from MeCN/ Et_2O to yield an analytical sample. Anal. Calcd for $\text{C}_{24}\text{H}_{60}\text{N}_3\text{FeS}_8\text{W}_2$: C, 26.9; H, 5.65; N, 3.92; Fe, 5.22; W, 34.3; S, 23.9. Found: C, 26.6; H, 5.71; N, 3.91; Fe, 5.11; W, 33.6; S, 23.7.

$[\text{Et}_4\text{N}]_2[\text{Fe}(\text{WS}_4)_2]$. The solid compounds $[\text{Et}_4\text{N}]_2\text{WS}_4$ (2.0 g; 3.50 mmol) and $\text{FeSO}_4 \cdot 7\text{H}_2\text{O}$ (0.50 g; 1.80 mmol) were dissolved in H_2O (60 mL). The dark green crystalline product that separated quickly was isolated by filtration, washed with H_2O , and dried in vacuo. The yield was 1.48 g; 88%. Anal. Calcd for $\text{C}_{16}\text{H}_{40}\text{N}_2\text{FeS}_8\text{W}_2$: C, 20.4; H, 4.28; N, 2.98. Found: C, 20.2; H, 4.21; N, 2.91.

Results and Discussion

Syntheses of Complexes. Our general interest in the area of iron-molybdenum-sulfur chemistry, and particularly its relation to synthetic analogues for the molybdenum site of nitrogenase, prompted us to attempt the synthesis, purification, and additional characterization of the species $[\text{Fe}(\text{MoS}_4)_2]^{2-}$, which had been briefly described¹⁶ by Müller and Sarkar. The solid that precipitated from an aqueous reaction mixture containing 2 equiv of $[\text{Et}_4\text{N}]_2[\text{MoS}_4]$ and 1 equiv of FeSO_4 in fact does have elemental analytical data roughly consistent with the formulation $[\text{Et}_4\text{N}]_2[\text{Fe}(\text{MoS}_4)_2]$. The complex, however, exhibits an infrared spectrum that is broad and unresolved in the Mo=S region and is nearly insoluble in solvents like MeCN and DMF, which readily dissolve other monomeric (but polynuclear) Fe-Mo-S complexes of this type. These facts led us to agree with Müller that this complex, at least as formed in aqueous solution, was polymeric in nature and of limited interest to us.

Because most of the known, well-characterized Fe-Mo-S complexes were prepared in nonaqueous solution, we decided to attempt the synthesis of $[\text{Fe}(\text{MoS}_4)_2]^{2-}$ under these conditions. Thus we reacted an iron(II) dithiolate species, $\text{Fe}(\text{S}_2\text{CNC}_5\text{H}_{10})_2$, with $[\text{Et}_4\text{N}]_2[\text{MoS}_4]$ in CH_2Cl_2 as shown in eq 2 hoping for a straightforward substitution reaction of bidentate sulfur-donor ligands on iron, i.e., tetrathiomolybdate



from the reaction mixture proved to be $[\text{Et}_4\text{N}]_3[\text{Fe}(\text{MoS}_4)_2]$ (1) and not the anticipated salt of the 2- trinuclear species. The fact that the isolated anion is trinegative indicates that reduction of the overall system has occurred. Possible reductants are the displayed dithiocarbamate ligands and the Fe(II) complex itself, but we have thus far not been able to identify the species responsible for reduction. It is, in fact, fortunate that 1 is relatively insoluble in CH_2Cl_2 , crystallizing from the reaction mixture and facilitating its isolation. We have been unable to isolate any other characterizable metal-containing products from the very dark filtrate and could not even identify 1 as a product when the reaction was run in MeCN, where the reaction mixture remains homogeneous.

The tungsten analogue of 1, $[\text{Et}_4\text{N}]_3[\text{Fe}(\text{WS}_4)_2]$ (2), was prepared analogously with one important exception. When $\text{Fe}(\text{S}_2\text{CNC}_5\text{H}_{10})_2$ and $[\text{Et}_4\text{N}]_2\text{WS}_4$ were reacted in CH_2Cl_2 alone, only a very slow reaction occurred. Addition of H_2O (10% by volume) greatly increased the rate of formation of 2, which, like its molybdenum analogue, precipitated from the reaction mixture. The H_2O may simply solubilize the WS_4^{2-} entity, facilitating its reaction with $\text{Fe}(\text{S}_2\text{CNC}_5\text{H}_{10})_2$, even though the mixture contains two distinct phases. As found for the analogous molybdenum system, the product yield is only ~40–50%, and no characterizable products could be isolated from the reaction-mixture filtrate, again making the nature of the reductant uncertain.

The $[\text{Ph}_4\text{P}]^+$ salt of $[\text{Fe}(\text{WS}_4)_2]^{2-}$ was previously¹⁶ isolated by Müller and Sarkar after reaction of $(\text{NH}_4)_2\text{WS}_4$ with FeSO_4 in the presence of hydrazine. We have prepared the $[\text{Et}_4\text{N}]^+$ salt of this anion, $[\text{Et}_4\text{N}]_2[\text{Fe}(\text{WS}_4)_2]$ (3), by a somewhat simpler procedure, i.e., mixing $[\text{Et}_4\text{N}]_2\text{WS}_4$ and FeSO_4 in H_2O with the product readily crystallizing from the aqueous reaction mixture. Since no reduction is necessary to produce the desired product, the use of hydrazine appears to be unnecessary. In fact, on the basis of the cyclic voltammetry studies of the $[\text{Fe}(\text{WS}_4)_2]^{3-/2-}$ complexes (see later), it is somewhat surprising that the reduced (3-) species was not isolated from a reaction mixture containing hydrazine.

While this paper was being prepared, Coucouvanis and co-workers reported¹⁷ the preparation of 3 by a method similar to that described herein and the synthesis of 2 by reduction of 3 with $[\text{Et}_4\text{N}]\text{BH}_4$. These workers also found that 3 forms adducts with coordinating solvents and determined the structure of the $[\text{Fe}(\text{WS}_4)_2(\text{DMF})_2]^{2-}$ ion. We were not aware of this latter reactivity, but our spectral and electrochemical results (vide infra) are not inconsistent with theirs.

Infrared and Visible Spectral Characterization. The infrared spectra of 1, 2, and 3 are particularly useful in evaluating their purity and assigning their structure. As seen in Figure 2a–c, very clean, well-resolved spectra are observed for the pure complexes. These spectra can be compared to that of “ $[\text{Et}_4\text{N}]_2[\text{Fe}(\text{MoS}_4)_2]$ ” shown in Figure 2d. In the case of this less well-defined species, the Mo-S bands (and the spectrum in general) are significantly broader, possibly indicating some type of polymerization. The actual M-S terminal and bridging band positions for 1, 2, and 3 are found in Table I with the assignments completely consistent with the previous¹⁸ detailed analysis carried out on the ion $[\text{Zn}(\text{WS}_4)_2]^{2-}$. It should be noted that the two predicted terminal Mo-S bands are readily observed for 1 but that for 2 and 3 only one W-S terminal band is seen. The reason for this effect is unknown, but the

(16) Müller, A.; Sarkar, S. *Angew. Chem., Int. Ed. Engl.* 1977, 16, 705.

(17) Stremple, P.; Baenziger, N. C.; Coucouvanis, D. *J. Am. Chem. Soc.* 1981, 103, 4603.

(18) Paulat-Bösch, I.; Krebs, B.; Müller, A.; Koniger-Ahlborn, E.; Dornfeld, H.; Schultz, H. *Inorg. Chem.* 1978, 17, 1440.

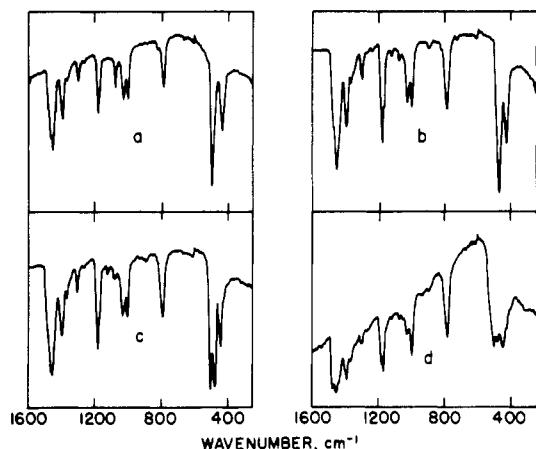


Figure 2. Infrared spectra as KBr disks of (a) $[\text{Et}_4\text{N}]_3[\text{Fe}(\text{WS}_4)_2]$, (b) $[\text{Et}_4\text{N}]_2[\text{Fe}(\text{WS}_4)_2]$, (c) $[\text{Et}_4\text{N}]_3[\text{Fe}(\text{MoS}_4)_2]$, and (d) $[\text{Et}_4\text{N}]_2[\text{Fe}(\text{MoS}_4)_2]$.

Table 1. Infrared and Electronic Spectral Data for 1, 2, and 3

complex	infrared data ^a	electronic data ^b
1	497 (s), ^c 486 (s) ^c 441 (m) ^d	630 sh (3000), 577 (7750) 507 (18 970), 409 (9150), 372 (16 070), 347 (26 920)
2	472 (s) ^c 431 (m) ^d	555 (4200), 492 (10 350), 434 (15 890), 360 (13 130)
3	495 (s) ^c 435 (m) ^d	613 (5230), 426 (9260) 375 (13 550)

^a Values in cm^{-1} . ^b Values in nm with molar absorptivities in parentheses. ^c Terminal M=S vibration. ^d Bridging $\text{M}(\mu\text{-S})_2\text{Fe}$ vibration.

same situation is observed (two M-S terminal bands for Mo and one for W) in the complexes $[\text{Cl}_2\text{FeS}_2\text{MS}_2]^{2-}$ and $[(\text{PhS})_2\text{FeS}_2\text{MS}_2]^{2-}$. It is also interesting to note that the terminal W-S band in 2 occurs at lower energy than the analogous band in 3. These relative band positions appear reasonable since the more reduced species (2) should have more electron density in the $\text{S}_2\text{MS}_2\text{FeMS}_2$ core, making the π -back-bonding of the terminal W-S moiety less effective. In fact, the lowering of the terminal W-S band by over 20 cm^{-1} from 3 to 2 could reflect the presence of formal W(V)-S units in 2, an observation that may be relevant to an understanding of the magnetic properties of this complex (vide infra).

The visible spectra of 1, 2, and 3 in MeCN solution are shown in Figure 3. All three complexes exhibit a number of sharp, well-resolved absorption peaks that are of practical use in determining purity and in identifying the species. While no detailed assignments of the visible bands have been attempted, it is of interest to draw some qualitative comparisons and conclusions in this area. For example, the spectra of 1 and 2 contain an almost identical manifold of peaks with that of the tungsten species shifted to higher wavelength by ~ 65 nm, an observation also made by Coucouvanis and co-workers.¹⁷ Since the spectrum of unchelated WS_4^{2-} contains two $\text{S} \rightarrow \text{M}$ charge-transfer bands (277 and 392 nm) similarly displaced from those of free MoS_4^{2-} (321 and 472 nm), it seems reasonable to also tentatively assign the bands of 2 and 3 to $\text{S} \rightarrow \text{M}$ charge transfers. The complexity of the spectra as compared to those of the parent tetrathiometalates is no doubt due to the removal of tetrahedral symmetry on coordination of the MS_4^{2-} unit. Similar conclusions have been drawn for other Fe-Mo-S species.⁶ Finally, it should be noted that the spectrum of 1 is somewhat solvent dependent, having slightly different molar absorptivities in H_2O and NMF than in MeCN. However, the general, very characteristic manifold of peaks for this species is present in these solvents, indicating

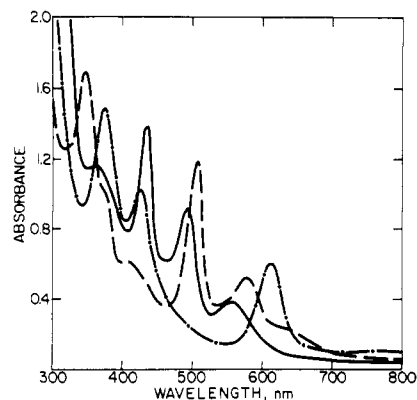


Figure 3. Visible spectra in MeCN solution of (a) $[\text{Et}_4\text{N}]_3[\text{Fe}(\text{MoS}_4)_2]$ (—), (b) $[\text{Et}_4\text{N}]_2[\text{Fe}(\text{WS}_4)_2]$ (---), and (c) $[\text{Et}_4\text{N}]_3[\text{Fe}(\text{WS}_4)_3]$ (—).

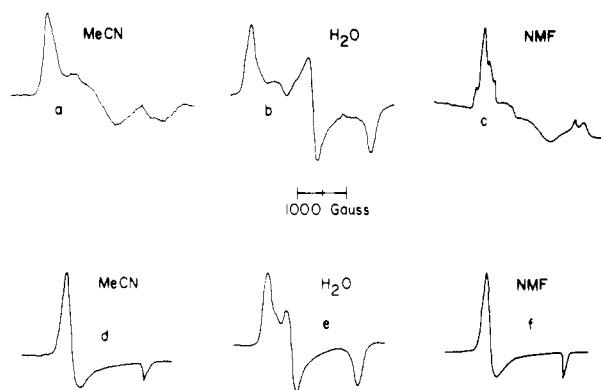


Figure 4. EPR spectra of $[\text{Et}_4\text{N}]_3[\text{Fe}(\text{MS}_4)_2]$ in various solvents: a-c, M = Mo; d-f, M = W.

that no adduct formation takes place between solvent and 1, as was observed for 3 in DMF.¹⁷ It is also interesting that our visible spectrum of 3, obtained in MeCN, is very similar to that reported¹⁷ in CH_2Cl_2 , where presumably no adduct formation with solvent has occurred, indicating that no significant formation of $[\text{Fe}(\text{WS}_4)_2(\text{MeCN})_2]^{2-}$ takes place under these conditions.

EPR Spectra. The magnetic moments of 1 and 2 (3.9 and 3.7 μ_B , respectively) indicate that these species are characterized by three unpaired electrons. EPR spectra have been obtained from 1 and 2 in several solvents (Figure 4), and all the spectra can be interpreted in terms of a $S = 3/2$ spin system.¹⁹ In the absence of an external magnetic field, the four states of a $S = 3/2$ manifold are split into two Kramers doublets that are separated in energy by

$$\Delta = 2|D|(1 + 3\lambda^2)^{1/2}$$

All the resonances in Figure 4 can be interpreted as coming from the lower doublet of a spin system with a large, positive zero-field splitting, $D > 0$. In no case do we observe features that are attributable to transitions (i) between doublets or (ii) within the upper doublet. Result i suggests that in each case the zero-field splitting, Δ , is large compared to the microwave quantum ($h\nu_0$; $\nu_0 \approx 9.2$ GHz), and result ii suggests that the

(19) Complex 3 is formally an even-electron species and as such would not be expected to be EPR active even at liquid-helium temperatures. In fact, the EPR spectrum of the complex does contain a very weak signal with g values of 2.06, 2.04, and 2.01, which is observable in frozen MeCN solutions at 77 K. Semiquantitative integration of this signal, however, indicates that it accounts for less than 5% of the weighed sample, and therefore, it is probably due to some (as yet unidentified) minor impurity. It seems reasonable to assume that pure 3 is in fact EPR silent, as expected. Attempts to obtain a magnetic moment for 3 by the Evans method were thwarted by its apparent decomposition in MeCN (color change from green to reddish brown) under the concentrated conditions necessary for the determination.

Table II. EPR Spectral Data for $[\text{Et}_4\text{N}]_3[\text{Fe}(\text{MS}_4)_2]$ (M = Mo, W)

sample	solvent	λ	$g_3(\text{obsd}) \pm$		$g_2(\text{obsd}) \pm$		$g_1(\text{obsd}) \pm$	
			0.10	$g_3(\text{calcd})^a$	0.05	$g_2(\text{calcd})^a$	0.01	$g_1(\text{calcd})^a$
$[\text{Et}_4\text{N}]_3[\text{Fe}(\text{MoS}_4)_2]$	H ₂ O	0.23	5.15	5.11	2.52	2.56	1.71	1.71
	CH ₃ CN	0.058	<i>b</i>	4.31	3.67	3.63	1.97	1.97
		0.17	5.01	4.87	2.94	2.93	1.83	1.83
	NMF	0.07	4.38	4.38	3.42	3.55	2.06	1.96
		0.15	4.77	4.77	<i>b</i>	3.05	2.03	1.86
		0.29	5.31	5.31	2.72	2.22	<i>b</i>	1.57
	0.30	5.86	5.86	<i>b</i>	2.17	<i>b</i>	1.54	
$[\text{Et}_4\text{N}]_3[\text{Fe}(\text{WS}_4)_2]$	H ₂ O	0.075	4.70	4.41	3.39	3.52	1.99	1.96
	CH ₃ CH	0.0	3.86	3.98	3.86	3.98	2.04	1.99
	NMF	0.0	3.96	3.98	3.96	3.98	2.06	1.99
		0.06	4.32	4.33	3.65	3.61	2.01	1.97

^a Calculated for the equations: $g_1 = g_z(2/(1 + 3\lambda^2)^{1/2} - 1)$, $g_2 = g_x(1 + (1 - 3\lambda)/(1 + 3\lambda^2)^{1/2})$, $g_3 = g_y(1 + (1 + 3)/(1 + 3\lambda^2)^{1/2})$, $g_x = g_y = g_z = 1.99$ (Hoffman, B. M.; Weschler, C. J.; Basolo, F. *J. Am. Chem. Soc.* 1976, 98, 5473-5481). These equations assume $\Delta \gg h\nu$, and the differences between $g_3(\text{calcd})$ may reflect a partial breakdown of assumption. ^b Not resolved (see Figure 4 and text).

upper doublet is unpopulated at 4.2 K and thus that $\Delta/k_B \gg T = 4.2$ K in all instances. This is consistent with the results of Simopoulos et al.,^{10b} who estimated $D \sim 5$ K from Mössbauer and magnetic susceptibility measurements.

The simplest spectra are those obtained from compound **2** dissolved in acetonitrile and NMF (Figure 4d,f). The observed g values of $g = 4$ and $g = 2$ are characteristic of an $S = 3/2$ system with a large axial zero-field splitting, namely with $D > 0$ and $\lambda = 0$. An additional weak and unidentified feature at $g \approx 7.5$ -8.0 in Figure 4d might be due to a two-quantum interdoubt transition but more likely is due to an impurity. The spectrum of **2** in water is slightly more complex, consisting of a major spectral component and other minor features (Figure 4e). The g -perpendicular region of the main spectrum is split around $g = 4$ (Table II), indicating a small rhombic distortion of the spin system that can be described by eq 1 with $\lambda = 0.075$. The additional weak features suggest the presence of minor amounts of other conformers and/or solvated forms of **2**.

The EPR spectrum of **1** in water is also relatively simple (Figure 4b) but very different from that of **2**. The main features, characterized by g values given in Table II, correspond to a highly rhombic $S = 3/2$ system, with $\lambda = 0.23$. Shoulders on the main features again suggest the presence of minor amounts of other forms of the center. In contrast, the spectrum of **1** in acetonitrile arises from two forms of the center having approximately equal concentrations (Figure 4a). Both forms have rhombic splittings, but neither has as large a value of λ as that seen in H₂O. In *N*-methylformamide, at least four species are identifiable by the features seen in the low-field region of the spectrum, Figure 4c. Two of the species in NMF appear to be similar to those seen in CH₃CN, as judged by the distortion parameter λ , and there are two species with very large values of E/D as well (Table II). The fact that the multiple-species spectra are only seen in weakly coordinating solvents suggests that the origin of the different forms arises from equilibria between different types of solvation about **1**. Thus, the addition of a strongly coordinating solvent such as pyridine might be expected to displace the weakly bound ligands and dramatically sharpen the spectrum. Unfortunately, the spectrum of **1** both in neat pyridine and in a medium of 5% pyridine in MeCN still exhibited a complex pattern of resonances. Further studies to identify the nature of the multiple species were not conducted.

In summary, both the Mo and W clusters, **1** and **2**, exhibit an $S = 3/2$ ground state with large zero-field splittings, and the properties of both clusters are highly solvent dependent. In a given solvent, the zero-field-splitting tensor has a more rhombic character for **1** than for **2**, and the rhombicity is larger in water than in acetonitrile and NMF.

The $S = 3/2$ state could arise from several formal metal-metal oxidation-state assignments, including the one with two

diamagnetic M(VI) species and an $S = 3/2$ Fe(I) noted in ref 10b. In principle, ferromagnetic coupling among the two M(V)'s and a low-spin, $S = 1/2$, Fe(III) could give an $S = 3/2$ ground state. However, the Mössbauer isomer shift of **1** is somewhat indicative of Fe(III),^{10b} a tetrahedral FeS₄ is unlikely to be low spin, and ferromagnetic coupling in such clusters is improbable. Rather, antiferromagnetic coupling of a high-spin ($S = 5/2$) Fe(III) to two $S = 1/2$ M(V) entities seems likely to underlie the magnetic properties of **1** and **2**. Antiferromagnetic coupling between iron and molybdenum has also been invoked⁶ to explain the magnetic properties of the complex ion $[\text{Fe}_2\text{MoS}_6(\text{SPh})_2]^{3-}$. If the two M(V) species are assumed to be equivalent, then the (FeM₂) spin-coupling problem is straightforward,²⁰ and the resulting wave functions can be used to obtain the correspondence between the observed spin-Hamiltonian parameters for the net cluster spin and the parameters characterizing the spin Hamiltonian of the individual ions. In this fashion, denoting the parameters of the individual ions by subscripts, we find

$$D = {}^{28}/_{15}D_{\text{Fe}} \quad E = {}^{28}/_{15}E_{\text{Fe}} \quad A(\text{Mo}) = -1/5A_{\text{Mo}}$$

The first observation to be made is that the cluster zero-field terms are roughly double that of the Fe^{III}S₄ core, thus helping to rationalize what otherwise appears to be a rather large value of $\Delta > 10$ K.^{10b,21} The second is that the molybdenum hyperfine splitting in the cluster is 5-fold reduced from that expected for the individual M(V). This effect, along with the relatively broad EPR lines, explains the absence of ^{97,95}Mo hyperfine satellites.

The final observation is that the rhombicity of the cluster, λ , is equal to that of the ferric iron itself, λ_{Fe} . Thus, the differences in rhombicity between **1** and **2** directly reflect differences in the geometry of the iron ion and the variations of λ from one solvent to another and between the different species observed in some solvents, e.g., NMF, reflect perturbations of the cluster geometry. These may be caused by direct interactions of the solvent with Fe but could need only reflect changes in geometry that are transmitted to the Fe. The high degree of rhombicity shown by **1** dissolved in H₂O is reminiscent of the rubredoxin FeS₄ center, for which $\lambda_{\text{Fe}} = 0.28$.²²

- (20) The intermediate spin S_1 formed by coupling the two M(V) spins is a good quantum number, and the total spin is obtained by antiferromagnetically coupling S_1 with $S_{\text{Fe}} = 5/2$. Only $S_1 = 1$ gives a cluster spin of $S = 3/2$.
- (21) Spin-spin dipole interactions are far too small to contribute significantly to D and E , and small solvent-induced differences between the two M species cannot contribute at all.
- (22) (a) Moura, I.; Huynh, B. H.; Hausinger, R. P.; LeGall, J.; Xavier, A. V.; Münck, E. *J. Biol. Chem.* 1980, 255, 2493. Moura, I.; Xavier, A. V.; Cammack, R.; Bruschi, M.; LeGall, J. *Biochim. Biophys. Acta* 1978, 533, 156. (b) Müller, A.; Mohan, N.; Bögggs, H. Z. *Naturforsch., B: Anorg. Chem., Org. Chem.* 1978, 33B, 978.

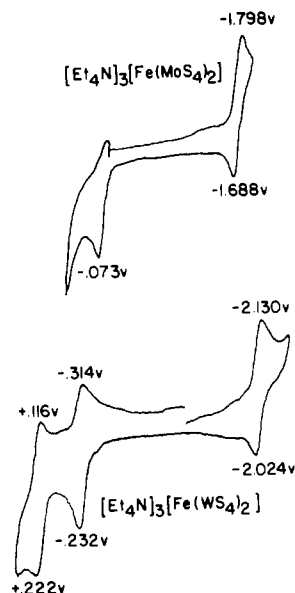


Figure 5. Cyclic voltammograms of $\sim 10^{-3}$ M solutions of $[\text{Et}_4\text{N}]_3[\text{Fe}(\text{MS}_4)_2]$ ($\text{M} = \text{Mo}, \text{W}$) in MeCN.

Electrochemistry. Cyclic voltammograms of **1** and **2** are shown in Figure 5. As reported previously,⁹ **1** undergoes a quasi-reversible reduction at ~ -1.75 V and an irreversible oxidation at ~ -0.07 V. Although controlled-potential coulometry studies have not been carried out, we tentatively assign the former couple to the reduction of $[\text{Fe}(\text{MoS}_4)_2]^{3-}$ to its 4-analogue and the latter oxidation to the formation of $[\text{Fe}(\text{MoS}_4)_2]^{2-}$, whose apparent lack of stability seems consistent with the irreversibility of the couple.

The voltammogram of **2** is indicative of the greater thermal stability of the various oxidation levels of this complex as compared to that of its molybdenum analogue. Here, three quasi-reversible waves (~ -2.05 , -0.27 , and $+0.17$ V) are observed and are tentatively assigned to the 3-/4-, 2-/3-, and 1-/2- couples of **2**, respectively. The reversibility of the 2-/3- couple for the tungsten complex is contrasted with the irreversibility for its molybdenum analogue and is consistent with the ease of isolation of $[\text{Fe}(\text{WS}_4)_2]^{2-}$, as shown in prior papers^{16,17} and in this work. In fact, the reversibility of the 1-/2- couple for **2** implies the existence of the complex $[\text{Fe}(\text{WS}_4)_2]^-$, but so far we have been unsuccessful in our attempts to isolate it. Except for its rest potential, the cyclic voltammogram of **3** is identical with that of **2** within experimental error, showing the electrochemical interconvertibility of these complexes. Our cyclic voltammograms of **2** and **3** in MeCN show a value for the proposed 2-/3- couple similar to that reported¹⁷ in CH_2Cl_2 by Coucouvanis and co-workers. As with the visible spectral studies, this result is consistent with no significant formation of a solvent adduct of **3** at these concentrations. Preliminary cyclic voltammetry studies of **3** in DMF indicate that each of the couples in Figure 5 is shifted to more negative potentials by ~ 0.15 V, a result consistent with the presence of $[\text{Fe}(\text{WS}_4)_2(\text{DMF})_2]^{2-}$.

Two principal conclusions come from the cyclic voltammetry studies. First, the positions of the 3-/4- and 2-/3- couples are at significantly more negative potential for tungsten as compared to those for molybdenum. This result is certainly not unexpected since it is normally more difficult to chemically reduce tungsten species than it is their molybdenum analogues. More significant perhaps is the dramatic difference in the reversibility of the electrochemical behavior for the molybdenum and tungsten species. The reversible couples observed for **2** are no doubt due to the greater thermal stability of $[\text{Fe}(\text{WS}_4)_2]^{2-}$ (and apparently its 1- analogue), but the reasons for this stability are not understood. Perhaps the WS_4 unit

is softer and forms stronger FeS_2M bridges than does MoS_4 in these delocalized species, preventing the dissociation of the complex under oxidizing conditions. Whatever the reason, it should be noted that we have also been unable to prepare pure $[\text{Co}(\text{MoS}_4)_2]^{2-}$, the molybdenum analogue of the well-known and easily synthesized^{22b} $[\text{Co}(\text{WS}_4)_2]^{2-}$. This result indicates that the greater stability of complexes containing bidentate WS_4^{2-} as a ligand may, in fact, be a general trend.

Relevance to Nitrogenase. Simply because of the similarity of the EPR spectra of **1** and **2** to those of the molybdenum-iron protein ($[\text{Mo-Fe}]$) of nitrogenase and FeMo-co (Figure 1), the question arises as to the actual relevance of these compounds to the molybdenum site of that enzyme. More importantly, detailed analyses of the spectra both of the biological material² and of **1** and **2** can be carried out by using the energy levels of an $S = 3/2$ manifold. Nitrogenase is one of the few biological systems with this spin state, and its chemical simulation from elements known to be present at the molybdenum site of the enzyme is encouraging. Finally, the high value of the zero-field splitting of **1** and **2** is reminiscent of that obtained^{2b} for $[\text{Mo-Fe}]$, differentiating these Fe-Mo-S cluster-containing species from other simple transition-metal species, e.g., Cr(III) complexes,²³ which give rise to $S = 3/2$ EPR signals but are characterized by a much smaller (~ 0.5 cm^{-1}) value of the zero-field splitting. Is there a possibility then that an $\text{Fe}(\text{MoS}_4)_2$ unit is actually present in $[\text{Mo-Fe}]$?

There are two molybdenum atoms per molecule of MoFe, and provided that molybdenum is involved in the EPR center of that entity, these molybdenum atoms appear to be independent of each other. This conclusion arises from studies where the EPR signal of $[\text{Mo-Fe}]$ has been quantitated in terms of spins per mole of $[\text{Mo-Fe}]$ by double integration. These types of experiments were carried out initially by Orme-Johnson, Münck, and co-workers^{2b} in the 8–15 K range and more recently by Hoffman, Watt, et al.²⁴ between 2.8 and 4.2 K. Both studies showed that each mole of $[\text{Mo-Fe}]$ gives rise to two spins, and since each $S = 3/2$ spin unit should contribute one spin, each mole of MoFe must contain two independent $S = 3/2$ moieties. These $S = 3/2$ spin units must contain only a single molybdenum atom since there are only two in the protein. This conclusion is also directly reached in a recent ENDOR study of $[\text{Mo-Fe}]$ by Hoffman et al.,²⁵ who present the first evidence that Mo is integrated into the $S = 3/2$ unit. Complex **1** contains two molybdenum atoms per $S = 3/2$ unit, giving rise to a total of one spin per mole. If the two molybdenum atoms of $[\text{Mo-Fe}]$ were indeed part of an $\text{Fe}(\text{MoS}_4)_2$ unit, that protein would of necessity give rise to one spin per mole rather than the observed value of two. Thus, the available evidence is conclusive in excluding the presence of this unit per se in $[\text{Mo-Fe}]$. Rather, this compound provides one of the best prototypes to date with which to characterize the properties of and spin-coupling among tetrahedrally sulfur-coordinated iron and molybdenum ions in an $(\text{Fe}_x\text{Mo}_y\text{S}_z^*)$ cluster. Indeed, recent reports²⁶ of non-nitrogenase Fe-Mo-S proteins from *Desulfovibrio* bacteria exemplify the overall importance of developing spectroscopic probes for complexes of this type so that the biological centers may be easily identified.

(23) Hempel, J. C.; Morgan, L. O.; Lewis, W. B. *Inorg. Chem.* 1970, 9, 2064.

(24) Watt, G. D.; McDonald, J. W.; Euler, W.; Hoffman, B. M., manuscript in preparation.

(25) Hoffman, B. M.; Roberts, J. E.; Orme-Johnson, W. H. *J. Am. Chem. Soc.*, in press.

(26) Moura, J. J. G.; Xavier, A. V.; Bruschi, M.; Legall, J.; Hall, D. O.; Cammack, R. *Biochem. Biophys. Res. Commun.* 1976, 72, 782. Moura, J. J. G.; Xavier, A. V.; Bruschi, M.; Legall, J.; Cabral, J. M. P.; J. *Less-Common Met.* 1977, 54, 555. Moura, J. J. G.; Xavier, A. V.; Cammack, R.; Hall, D. O.; Bruschi, M.; Legall, J. *Biochem. J.* 1977, 173, 419. Hatchikian, E. C.; Bruschi, M. *Biochem. Biophys. Res. Commun.* 1979, 86, 725.

Acknowledgment. We thank Dr. J. E. Roberts for assistance with the EPR spectra. This work has been supported by Grant DMR 77-26409 from the Solid State Chemistry Division of the National Science Foundation (W.B.E.) to B.M.H. and by a grant from the donors of the Petroleum Research Fund, administered by the American Chemical Society, to B.M.H. The EPR measurements were performed in the magnetic resonance facility at the Northwestern University Materials

Research Center, supported in part by Grant DMR 76-80847 from the National Science Foundation NSF-MRL Program. The work was partially supported by a grant from the USDA/SEA Competitive Research Grants Office (59-2394-1-1-675-0) to J.W.M. and W.E.N.

Registry No. 1, 75282-37-0; 2, 86161-22-0; 3, 86161-23-1; [Et₄N]₂MoS₄, 14348-09-5; [Et₄N]₂WS₄, 14348-05-1; Fe(S₂CNC₅-H₁₀)₂, 75752-67-9.

Contribution from the Department of Chemistry, Faculty of Science, Tohoku University, Aoba, Aramaki, Sendai 980, Japan, and College of Medical Sciences, Tohoku University, Seiryomachi, Sendai 980, Japan

Redox Potentials and Related Parameters of Cobalt(III/II) Complexes Containing Aminopolycarboxylates

HIROSHI OGINO* and KAZUKO OGINO

Received November 2, 1982

The formal potentials, reaction entropies, and other thermodynamic parameters have been determined for 12 (aminopolycarboxylato)cobalt(III/II) redox couples in aqueous solutions. It has been shown that the magnitudes of free energies derived from formal potentials are determined primarily by the entropies rather than enthalpies. The entropy differences of the redox couples are dependent mainly on the charges of the complex ions: $-25 \pm 4 \text{ J K}^{-1} \text{ mol}^{-1}$ for [complex]⁻²⁻ (six complexes), $+15 \pm 5 \text{ J K}^{-1} \text{ mol}^{-1}$ for [complex]^{0/-} (four complexes), and $+54 \pm 16 \text{ J K}^{-1} \text{ mol}^{-1}$ for [complex]^{2+/-} (one complex) at $I = 0.1 \text{ M}$ and $25 \text{ }^\circ\text{C}$. The stability constants of several (aminopolycarboxylato)cobalt(III) complexes have also been obtained.

Introduction

The kinetics of redox reactions of metal complexes have been investigated extensively, and the importance of thermodynamic parameters in elucidating the mechanisms of the redox reactions has been well recognized.¹ Though there have been numerous studies of the kinetics of homogeneous redox reactions involving Co(III/II) complexes, the redox potentials of Co(III/II) couples have been reported for only a few complexes. This is mainly because of the irreversibility of the electrode processes and the lability of Co(II) complexes. In this work, however, a number of (aminopolycarboxylato)cobalt(III) complexes are found to be reduced reversibly at the mercury electrode and allow the determination of the formal redox potentials (E°) of the half-cell reactions



The entropy differences of the redox couples

$$\Delta S_{\text{rc}}^\circ = S^\circ(\text{Co}^{\text{II}}\text{L}) - S^\circ(\text{Co}^{\text{III}}\text{L}) \quad (2)$$

are also determined by measuring the temperature coefficients of nonisothermal electrochemical cells.² The factors that control the thermodynamic quantities—formal potentials, entropies, and enthalpies—of the (aminopolycarboxylato)cobalt(III/II) redox couples are examined by changing the nature of the coordinated ligands systematically.

Experimental Section

Materials. The solutions of sodium perchlorate and lithium perchlorate were prepared by treating the corresponding carbonate with an equivalent amount of 70% perchloric acid.

Two types of aminopolycarboxylates were used as ligands. One is tetraacetates and the other triacetates. The ligands and their abbreviations are given in Table I. The cobalt(III) complexes of these ligands were synthesized in the following procedures, were characterized by elemental analyses, and gave satisfactory results.

Table I. Structures and Abbreviations of Aminopolycarboxylates

Tetraacetates		
-R-	abbrevn	name
-(CH ₂) ₂ -	edta	1,2-diaminoethane- <i>N,N,N',N'</i> -tetraacetate
-(CH ₂) ₃ -	trdta	1,3-diaminopropane- <i>N,N,N',N'</i> -tetraacetate
-(CH ₂) ₄ -	tdta	1,4-diaminobutane- <i>N,N,N',N'</i> -tetraacetate
	pdta	1,2-diaminopropane- <i>N,N,N',N'</i> -tetraacetate
	ms-bdta	<i>meso</i> -2,3-diaminobutane- <i>N,N,N',N'</i> -tetraacetate
	cydta	<i>trans</i> -1,2-diaminocyclohexane- <i>N,N,N',N'</i> -tetraacetate
	dpot	1,3-diamino-2-propanol- <i>N,N,N',N'</i> -tetraacetate
Triacetates		
-R'	abbrevn	name
-H	edtra	1,2-diaminoethane- <i>N,N,N'</i> -triacetate
-CH ₃	medtra	1,2-diaminoethane- <i>N</i> -methyl- <i>N,N',N'</i> -triacetate
-(CH ₂) ₂ OH	hedtra	1,2-diaminoethane- <i>N</i> -hydroxyethyl- <i>N,N',N'</i> -triacetate
-(CH ₂) ₃ OH	hpedtra	1,2-diaminoethane- <i>N</i> -hydroxypropyl- <i>N,N',N'</i> -triacetate

* To whom correspondence should be addressed at the Department of Chemistry.

The following compounds were obtained by published procedures: K[Co(trdta)]·2H₂O,³ K[Co(tdta)]·3H₂O,⁴ K[Co(pdta)]·H₂O,⁵